Electronic Supplementary Information for

Oxygen migration and optical properties of the coronene oxides and their persulfurated derivatives: Insight into the electric field effect and the oxygen-site dependence

Qing Zhang, Yuanyan Li, and Zexing Cao*

State Key Laboratory of Physical Chemistry of Solid Surfaces and Fujian Provincial Key Laboratory of Theoretical and Computational Chemistry, College of Chemistry and Chemical Engineering, Xiamen University, Xiamen 360015, China

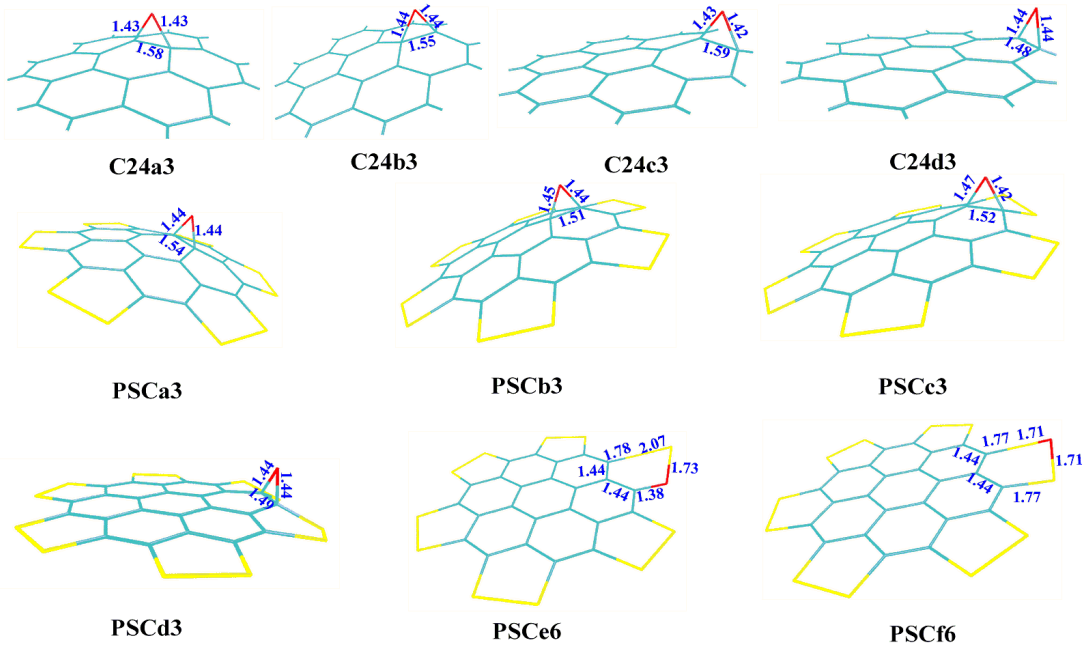

Fig. S1 The B3LYP-optimized structures of C24 epoxides and PSC oxides.

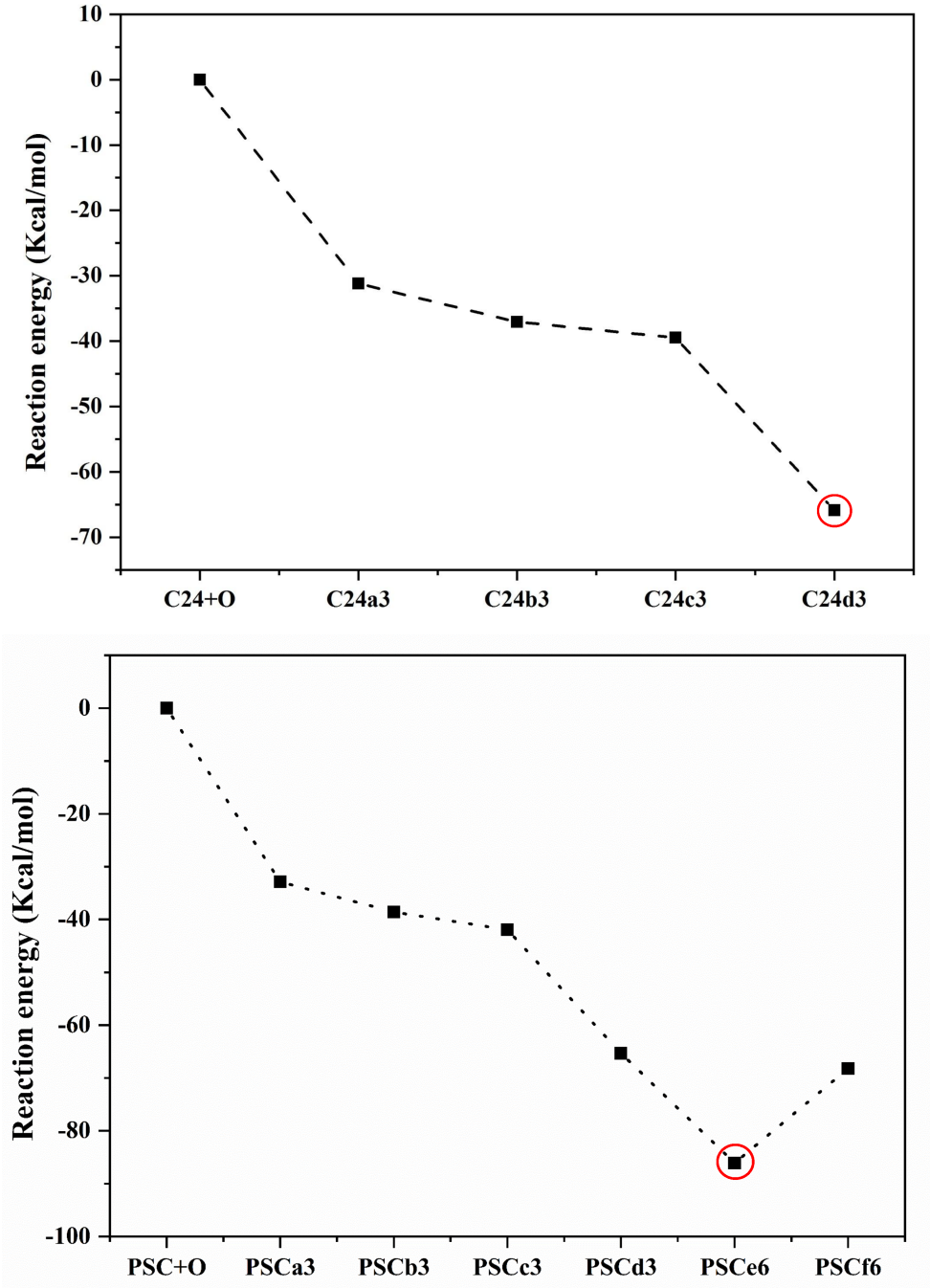

Fig. S2 Predicted related energies for the C24 epoxides and PSC oxides at the B3LYP/6-31G(d,p) level of theory.

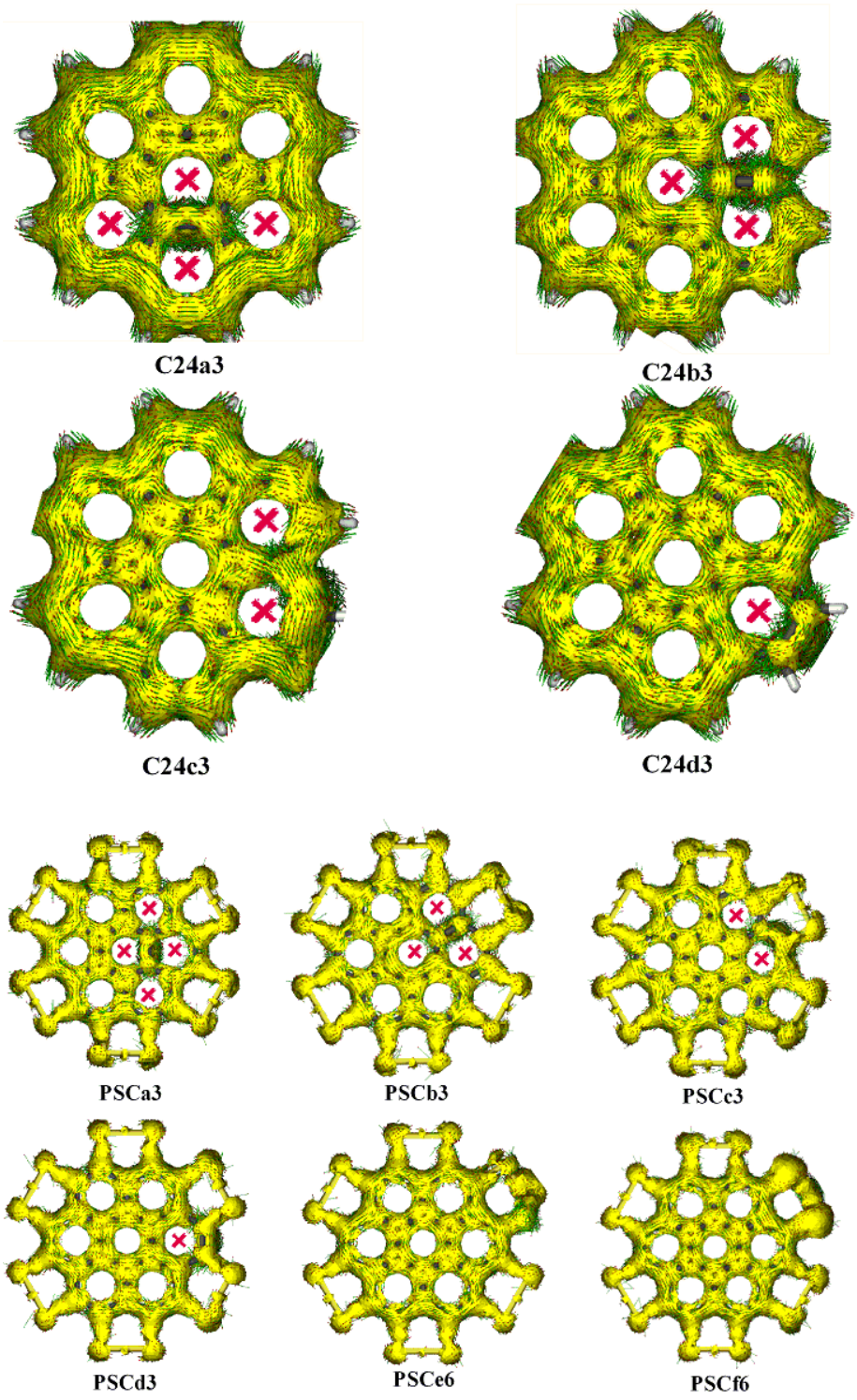

Fig. S3 The anisotropy of the induced current density (ACID) of the C24 epoxides and PSC oxides, where the red cross indicates the delocalization destruction of π electrons in the inner carbon ring induced by the epoxy group.

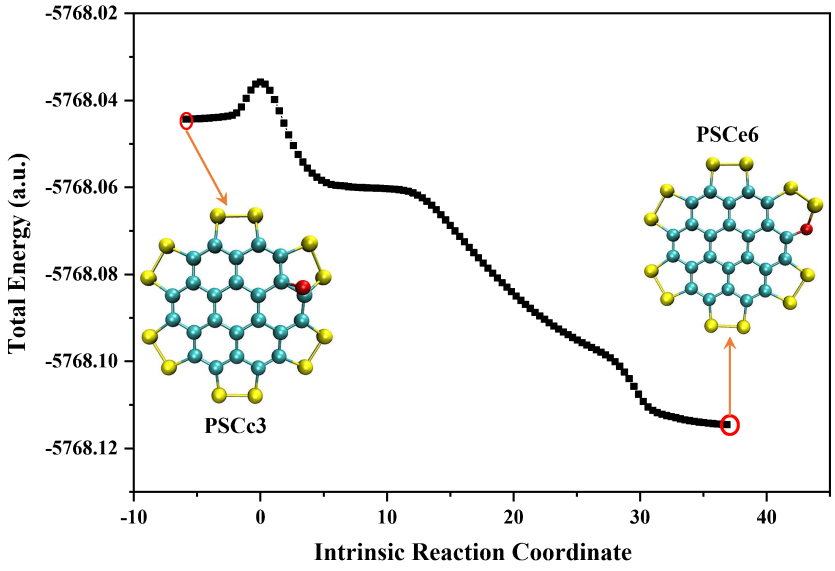

Fig. S4 Evolution of the total energy along IRC from PSCc3 to PSCe6.

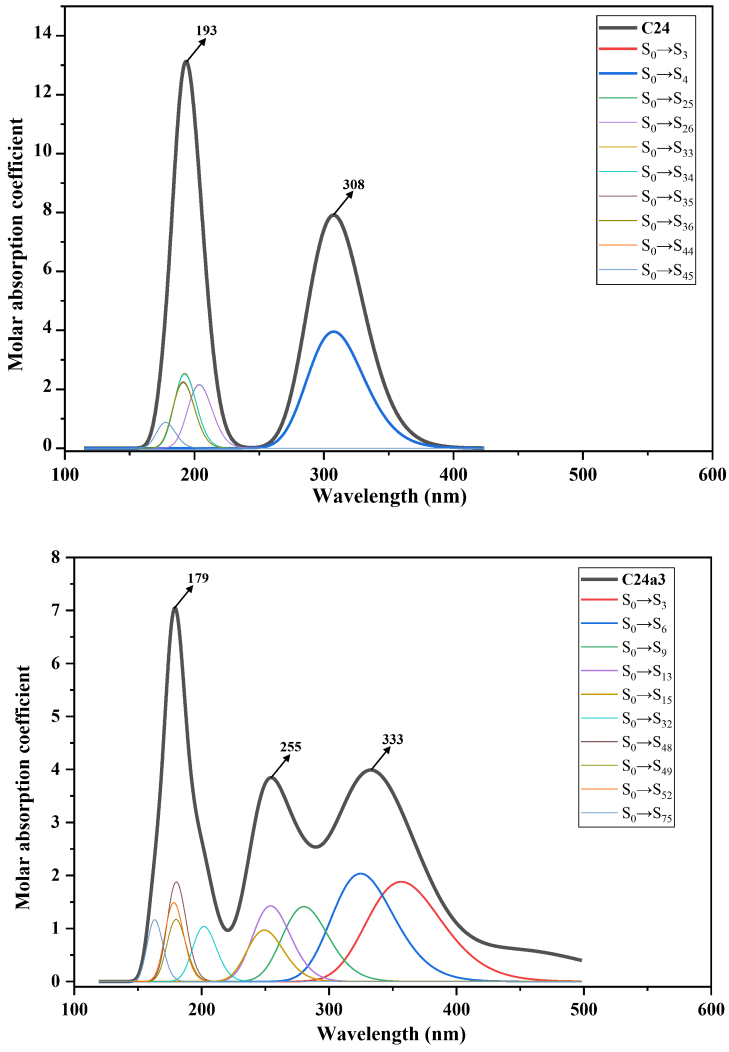

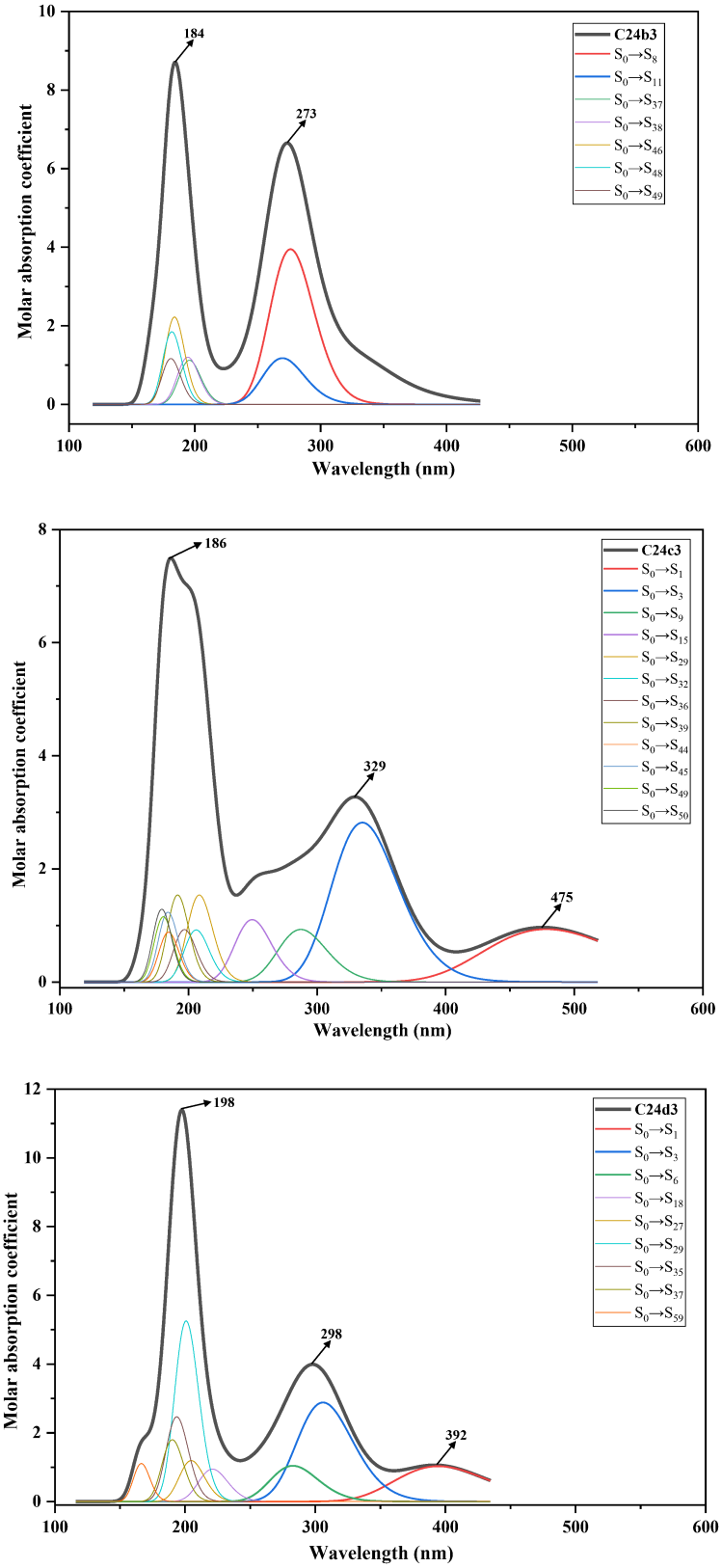

Fig. S5 The contribution of individual electronic transitions to the absorption spectra of C24 and C24 epoxides, respectively.

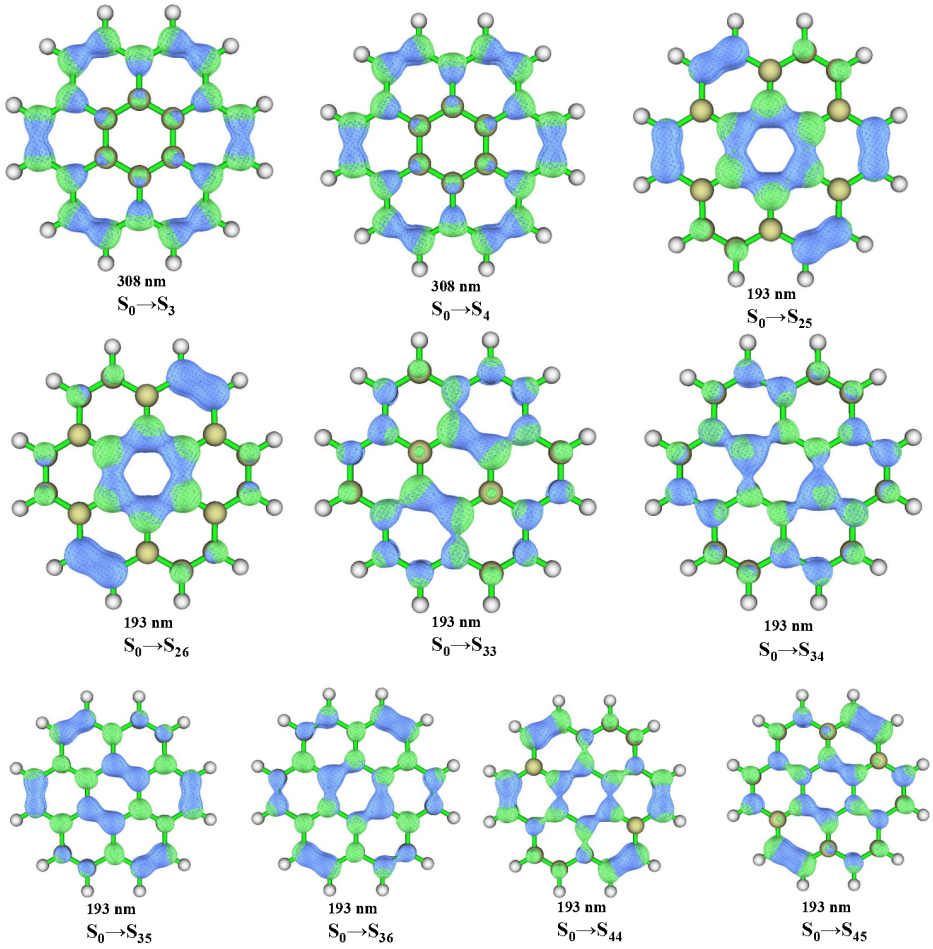

Fig. S6 Predicted electron-hole distributions of C24 at the S_0-state geometry, where blue and green isosurfaces represent hole and electron distributions here and in subsequent Figures, respectively.

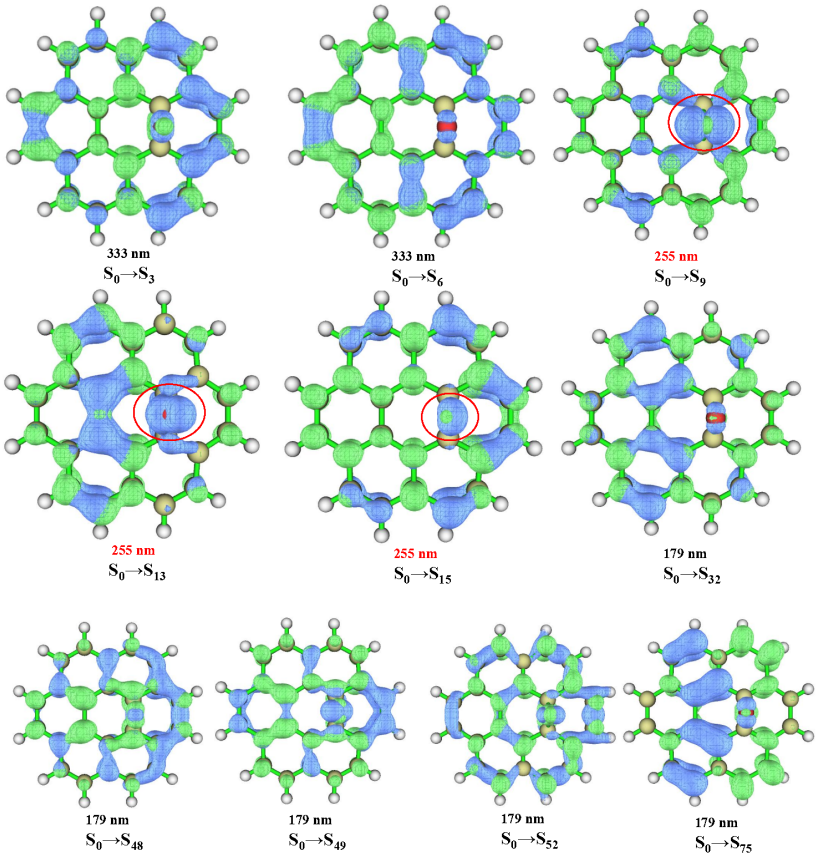

Fig. S7 Predicted electron-hole distributions of C24a3 at the S_0-state geometry.

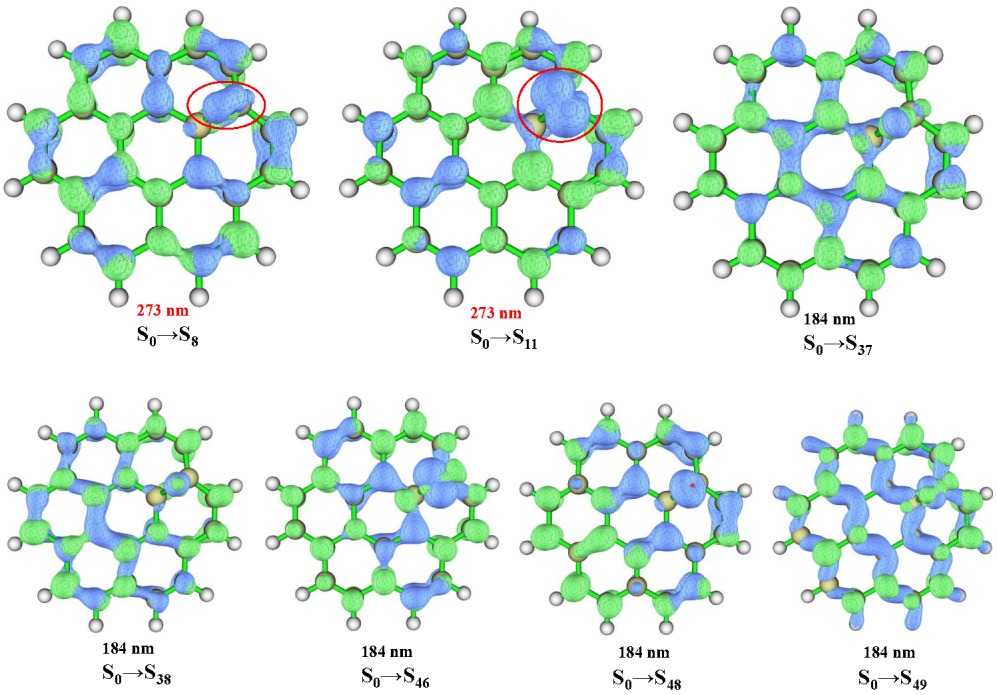

Fig. S8 Predicted electron-hole distributions of C24b3 at the S_0-state geometry.

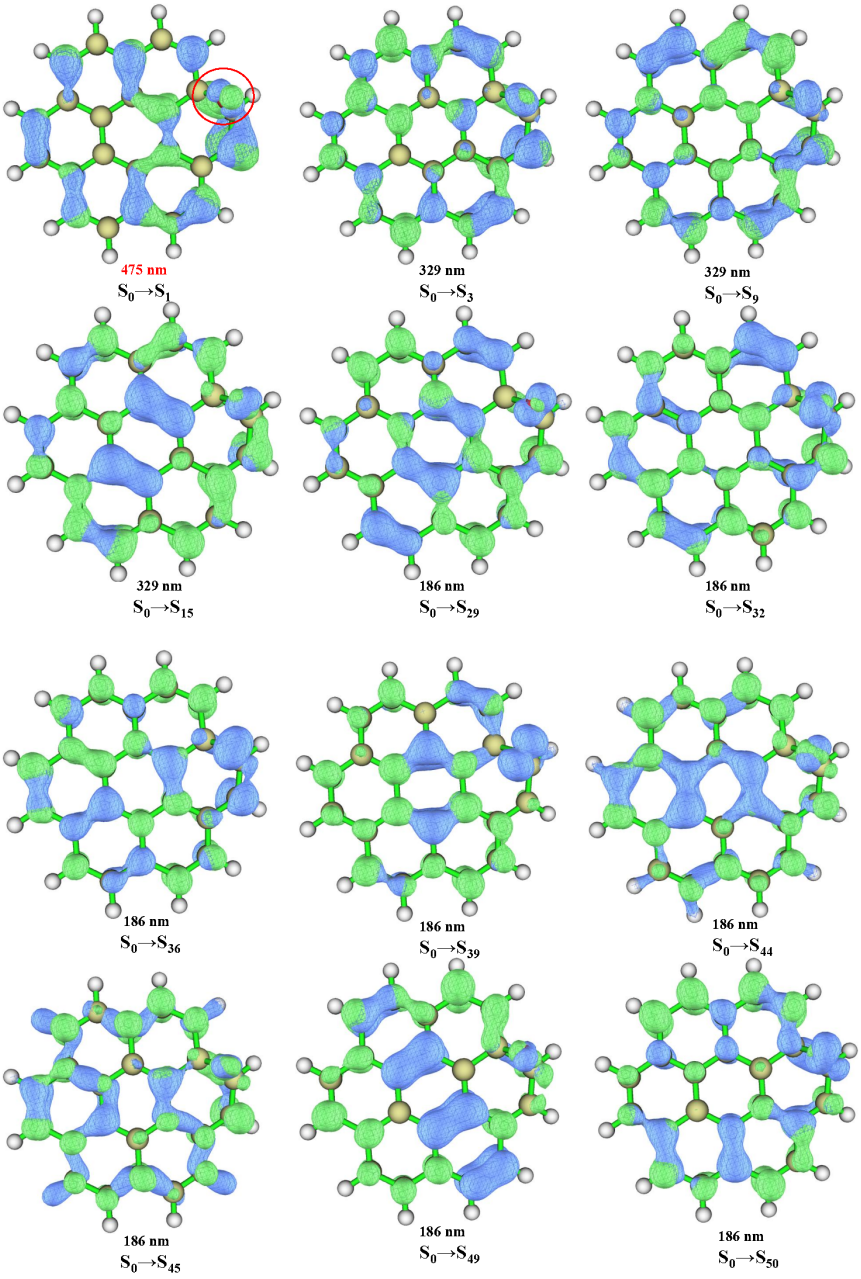

Fig. S9 Predicted electron-hole distributions of C24c3 at the S_0-state geometry.

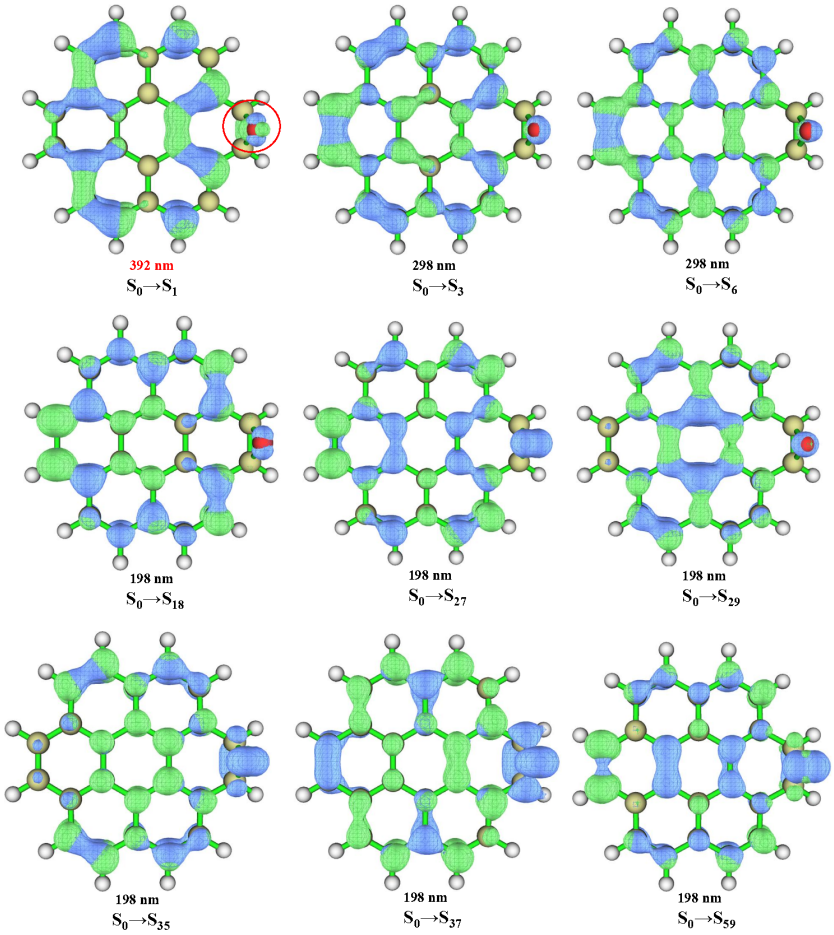

Fig. S10 Predicted electron-hole distributions of C24d3 at the S_0-state geometry.

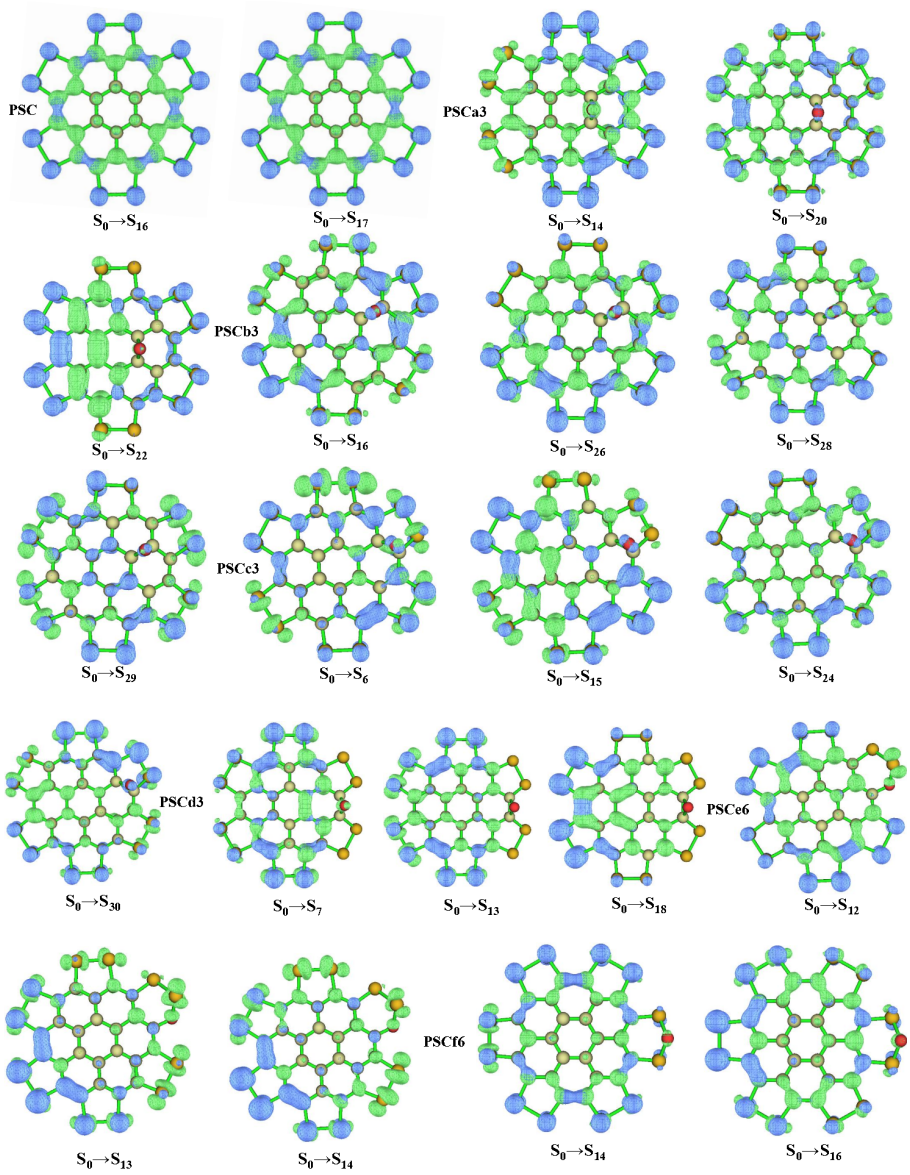

Fig. S11 Predicted electron-hole distributions of the low-energy transitions for PSC oxides and the pristine PSC, based on the S_0-state geometry.

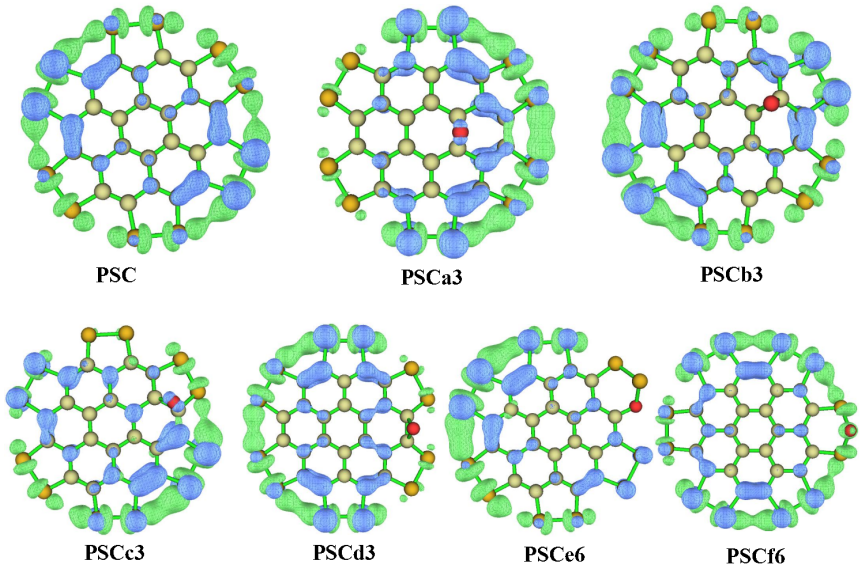

Fig. S12 Predicted electron-hole distributions of the $S_0 \rightarrow S_1$ transitions of the PSC oxides and the pristine PSC.

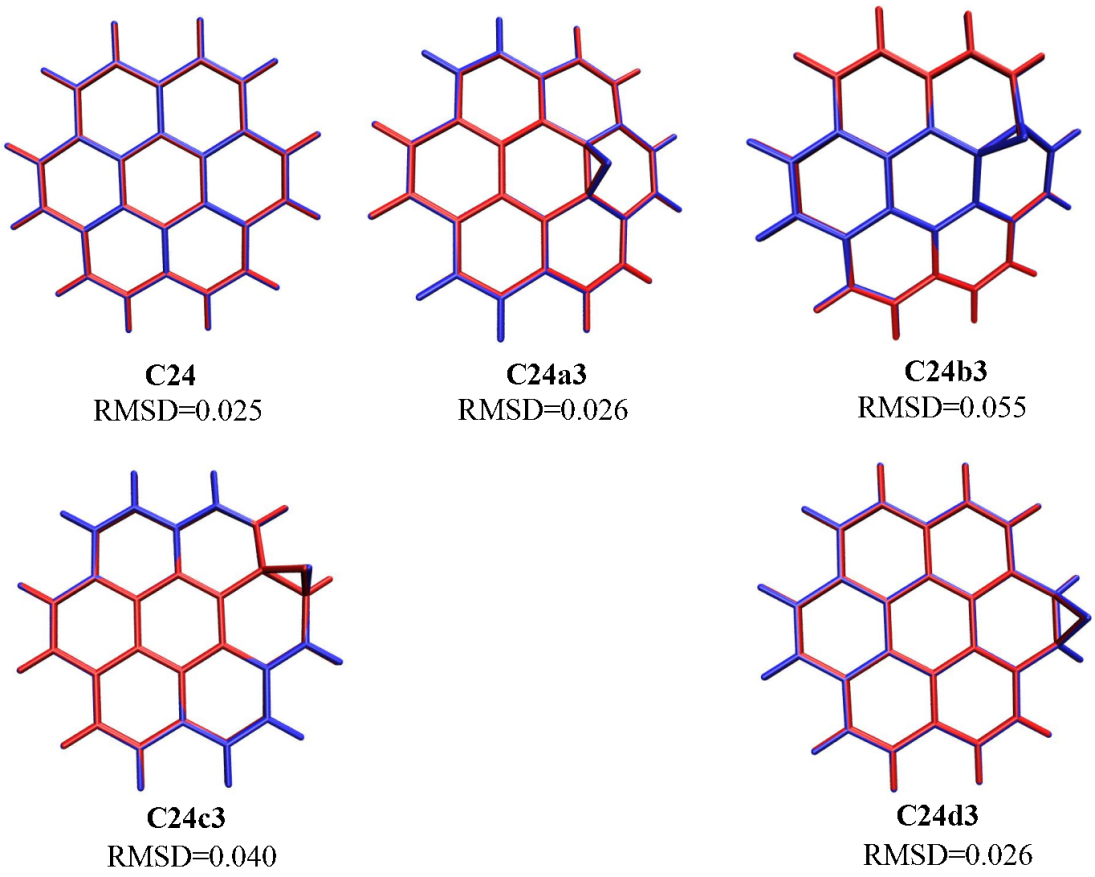

Fig. S13 Geometry comparison and RMSD values between the CIS (red) and TD-B3LYP optimized (blue) S_1 structures of C24 and its epoxides.

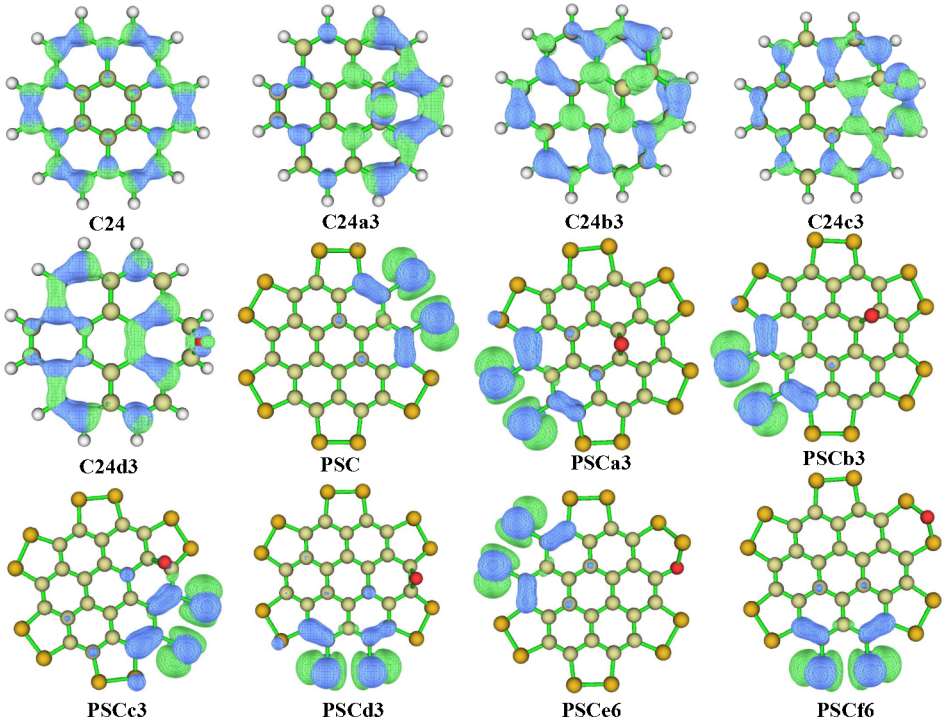

Fig. S14 Calculated electron-hole distributions of the $S_1 \rightarrow S_0$ transitions for C24 and PSC and their oxides, based on the relaxed S_1 geometry.

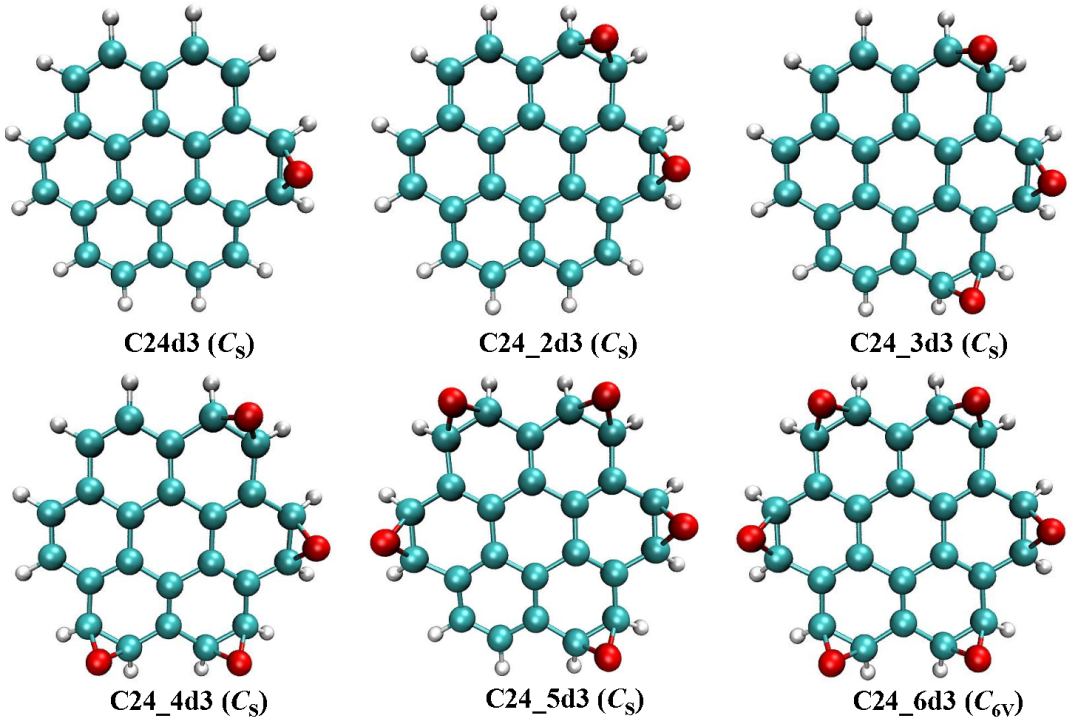

Fig. S15 Optimized S_1-relaxed structures of the C24 epoxides with multiple epoxy groups varying from 1 to 6 at the edge position, based on the rim-epoxidized C24d3, in which the molecular symmetry is measured by using Materials Studio software with a tolerance of 0.01 Å.

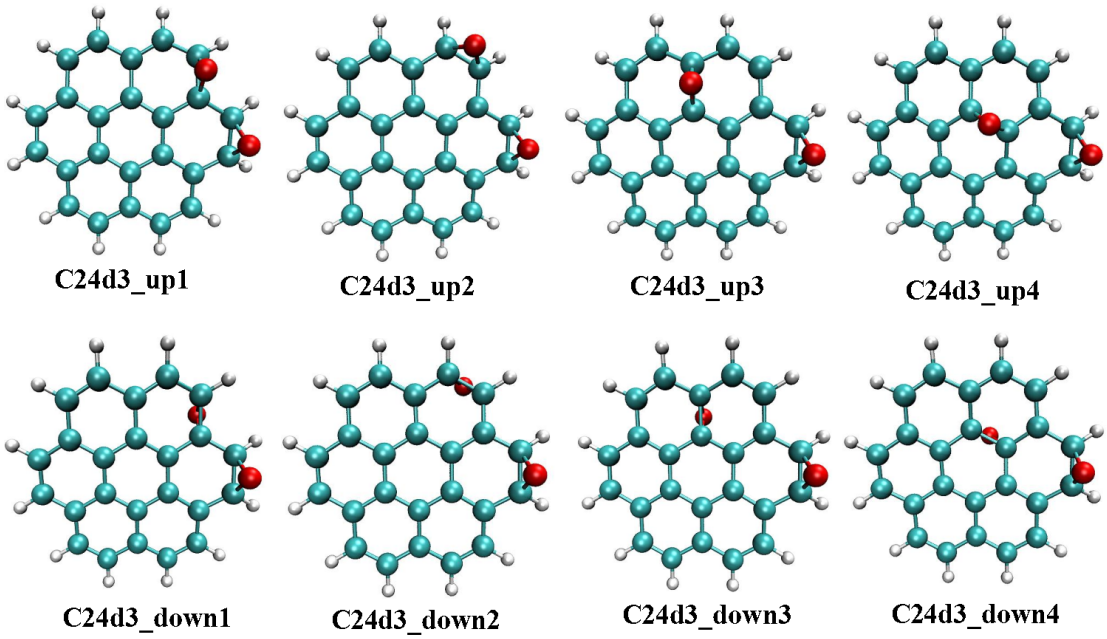

Fig. S16 The optimized structures of the C24 epoxides with double epoxy groups bonded on one side or both sides of the basal plane.

Table S1 The vertical emission energies (ΔE_{emi} and λ_{emi}), transition dipole moments (μ) and oscillator strength (f) of the PSC oxides and the pristine PSC predicted by the CIS approach.

Structure	E_{emi}(eV)	λ_{emi}(nm)	μ (Debye)	f ($S_1 \rightarrow S_0$)
PSC	0.98	1259	0.03	0.000
PSCa3	1.07	1159	0.16	0.001
PSCb3	1.11	1120	0.12	0.000
PSCc3	0.59	2117	0.11	0.000
PSCd3	0.95	1303	0.08	0.000
PSCe6	0.99	1254	0.03	0.000
PSCf6	1.01	1233	0.03	0.000

Table S2 The predicted vertical emission energies (ΔE_{emi} and λ_{emi}), transition dipole moments (μ), oscillator strengths (f), and the radiative (k_r) and non-radiative decay rates (k_{nr}) of the pristine C24 and C24 epoxides predicted by the ωB97XD/6-31g(d,p) method.

	ΔE_{emi} (eV)	λ_{emi} (nm)	μ (Debye)	$f(S_1 \rightarrow S_0)$	k_r (s^{-1})	k_{nr} (s^{-1})
C24	3.38	367	0.00	0.000	-	1.21×10^{8}
C24a3	2.31	537	3.58	0.112	2.60×10^{7}	3.96×10^{9}
C24b3	3.38	366	1.52	0.030	1.47×10^{7}	2.47×10^{10}
C24c3	2.22	559	4.14	0.144	3.07×10^{7}	6.84×10^{10}
C24d3	3.20	388	4.54	0.250	1.11×10^{8}	8.94×10^{7}

Table S3 The predicted vertical emission energies (ΔE_{emi} and λ_{emi}), transition dipole moments (μ), oscillator strength (f), and the radiative decay rate (k_r) and non-radiative rate (k_{nr}) of the C24 epoxides with the epoxy groups varying from 1 to 6.

Structure	ΔE_{emi} (eV)	λ_{emi}(nm)	μ (Debye)	f ($S_1 \rightarrow S_0$)	k_r (s^{-1})	k_{nr} (s^{-1})
C24d3	2.86	433	4.15	0.187	6.64×10^{7}	4.81×10^{6}
C24_2d3	2.59	480	3.63	0.129	3.75×10^{7}	9.65×10^{6}
C24_3d3	2.68	463	1.68	0.029	8.91×10^{6}	4.45×10^{8}
C24_4d3	2.53	491	1.27	0.016	4.29×10^{6}	9.80×10^{6}
C24_5d3	2.59	479	0.73	0.005	1.51×10^{6}	1.46×10^{8}
C24_6d3	2.55	486	0.00	0.000	-	1.26×10^{7}

Table S4 The predicted vertical emission energies (ΔE_{emi}, eV and λ_{emi}, nm), transition dipole moments (μ, debye) and oscillator strength (f) of the C24 epoxides with double epoxy groups bonded on one side or both sides of the basal plane.

Structure	ΔE_{emi}	λ_{emi}	μ	f	Structure	E_{emi}	λ_{emi}	μ	f
C24d3_up1	2.23	556	4.52	0.173	C24d3_down1	2.32	534	4.64	0.189
C24d3_up2	2.59	480	3.63	0.129	C24d3_down2	2.62	473	3.68	0.134
C24d3_up3	2.44	508	1.80	0.030	C24d3_down3	2.42	512	1.78	0.029
C24d3_up4	2.20	564	3.06	0.078	C24d3_down4	2.13	581	2.97	0.072